

Supporting information

**WO_x@PEDOT Core-Shell Nanorods: Hybrid Hole-Transporting
Materials for Efficient and Stable Perovskite Solar Cells**

Ping Liu,^{a,b} Chen Wang,^{a,b} Dongying Zhou,^{a,b} Quan Yuan,^{a,b} Yu Wang,^{a,b} Yao Hu,^{a,b} Dongwei
Han,^{a,b} Lai Feng^{a,b,*}

^a *Soochow Institute for Energy and Materials Innovations, College of Physics, Optoelectronics
and Energy, Soochow University, Suzhou 215006, China*

^b *Jiangsu Key Laboratory of Advanced Carbon Materials and Wearable Energy Technologies,
Soochow University, Suzhou 215006, China*

**Corresponding author (Tel: +86 512 65223650; E-mail address: fenglai@suda.edu.cn (Lai
Feng))*



Figure S1. Photos of the samples of WO_x NWs, WO_x@PEDOT and PEDOT:PSS.

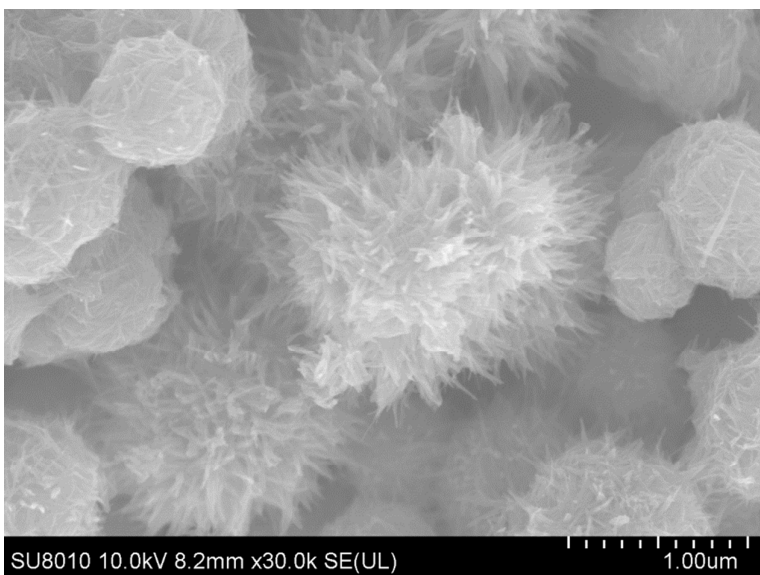


Figure S2. SEM image of as-prepared WO_x NWs.

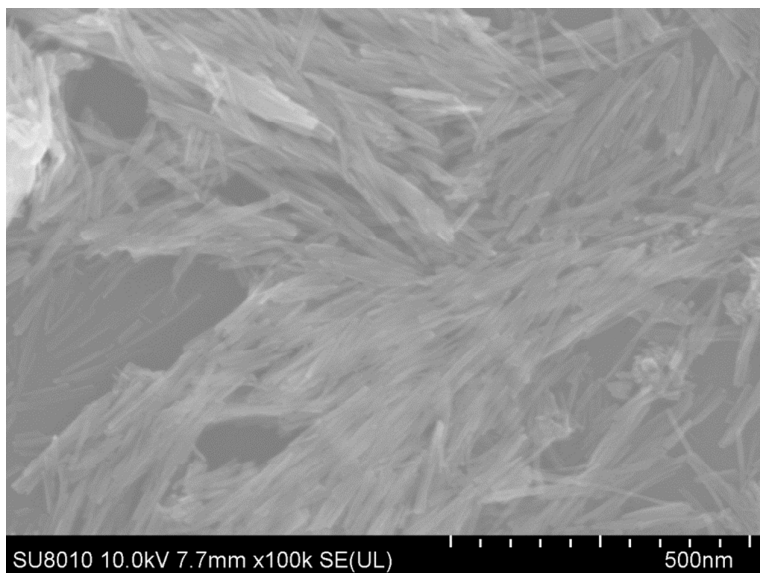


Figure S3. SEM image of WO_x NWs obtained after constant stirring in aqueous solution without EDOT.

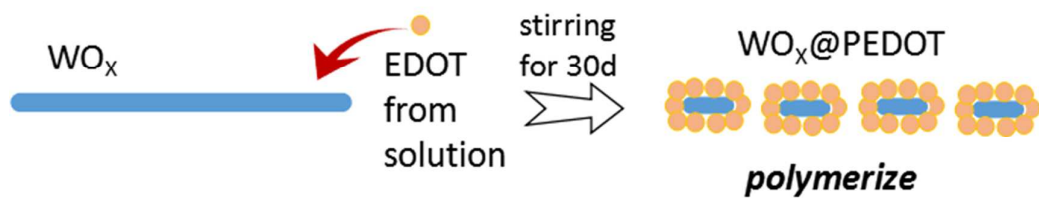


Figure S4. Schematic illustration of the truncation process to produce $\text{WO}_x\text{@PEDOT}$ NRs from WO_x NWs.

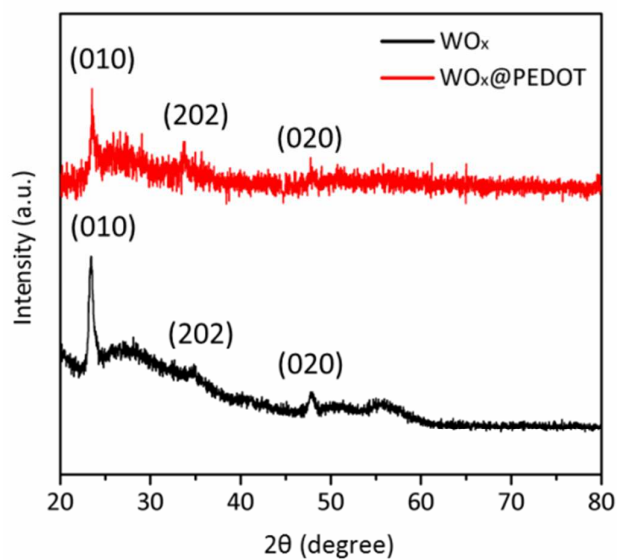


Figure S5. XRD patterns of WO_x NWs and $\text{WO}_x\text{@PEDOT}$ NRs.

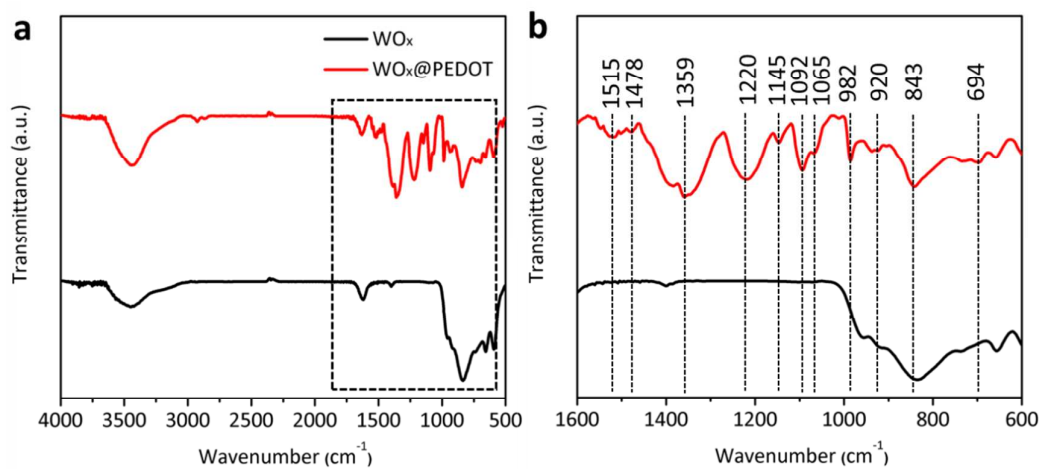


Figure S6. (a,b) FT-IR full and highlighted spectra of WO_x NWs and $\text{WO}_x\text{@PEDOT}$

NRs.

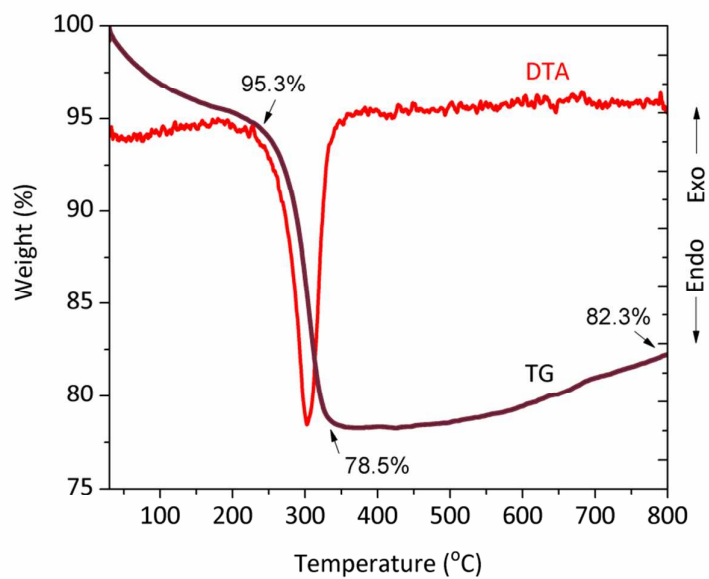


Figure S7. TGA profile of $\text{WO}_x\text{@PEDOT}$ NRs measured in air atmosphere.

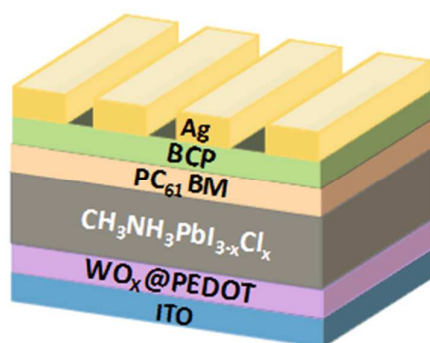


Figure S8. Device architecture of solution-processed planar p-i-n PeSC.

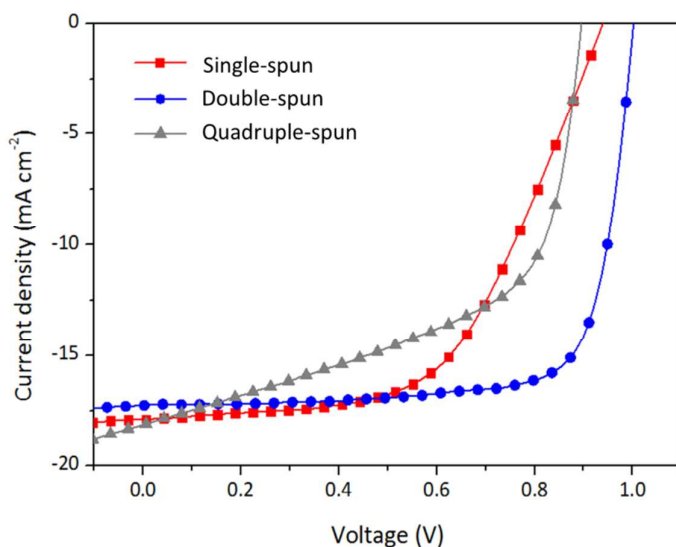


Figure S9. J - V curves of PeSCs containing single, double, and quadruple-spun WO_x @PEDOT layers.

Table S1. Photovoltaic parameters extracted from the devices containing single, double, and quadruple-spun WO_x @PEDOT layers.

HTL	V_{oc} (V)	J_{sc} (mA/cm ²)	FF(%)	PCE (%)
Single-spun WO_x @PEDOT layer	0.94	17.88	56.0	9.40
Double-spun WO_x @PEDOT layers	1.00	17.25	76.8	13.24
Quadruple-spun WO_x @PEDOT layers	0.89	18.08	56.1	9.04

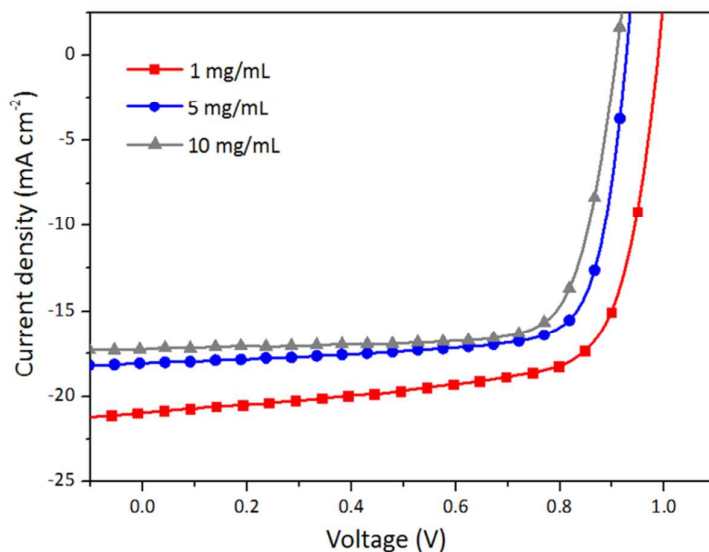


Figure S10. J – V curves of PeSCs with $\text{WO}_x\text{@PEDOT:PEDOT:PSS}$ prepared using the $\text{WO}_x\text{@PEDOT}$ solution with the concentration of 1 mg/mL, 5 mg/mL and 10 mg/mL.

Table S2. Photovoltaic parameters extracted from the devices with $\text{WO}_x\text{@PEDOT:PEDOT:PSS}$ prepared using the $\text{WO}_x\text{@PEDOT}$ solution with the concentration of 1 mg/mL, 5 mg/mL and 10 mg/mL.

$\text{WO}_x\text{@PEDOT}$ solution	V_{oc} (V)	J_{sc} (mA/cm ²)	FF (%)	PCE (%)
1 mg/mL	0.99	20.93	71.3	14.73
5 mg/mL	0.93	18.04	76.1	12.74
10 mg/mL	0.90	17.24	77.4	12.04

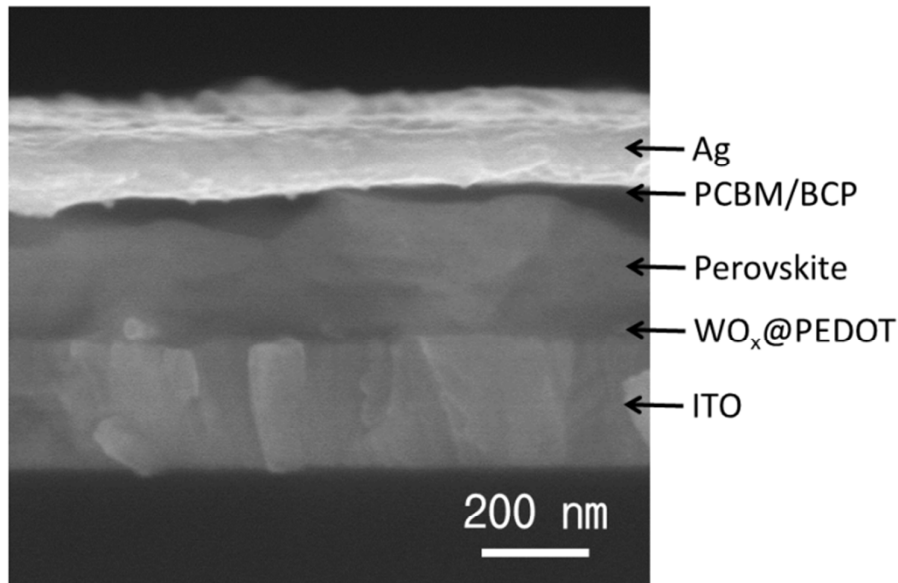


Figure S11. Cross-sectional SEM image of typical device with WO_x@PEDOT NRs.

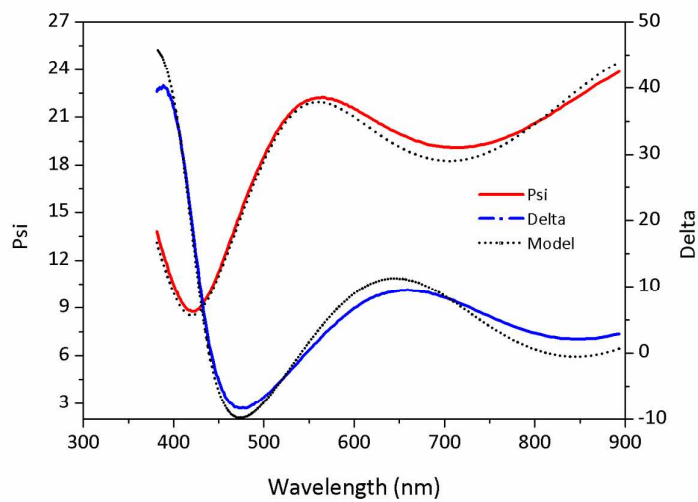


Figure S12. Ellipsometric raw data (i.e. Ψ and Δ) as a function of wavelength collected from ITO/WO_x@PEDOT film.

The optical models, representing the general structure of the tested samples, were built as “ITO(150 nm)/WO_x@PEDOT(Thickness, fit)” for. By fitting, the thickness of the WO_x@PEDOT HTL is estimated to be ca. 22 nm.

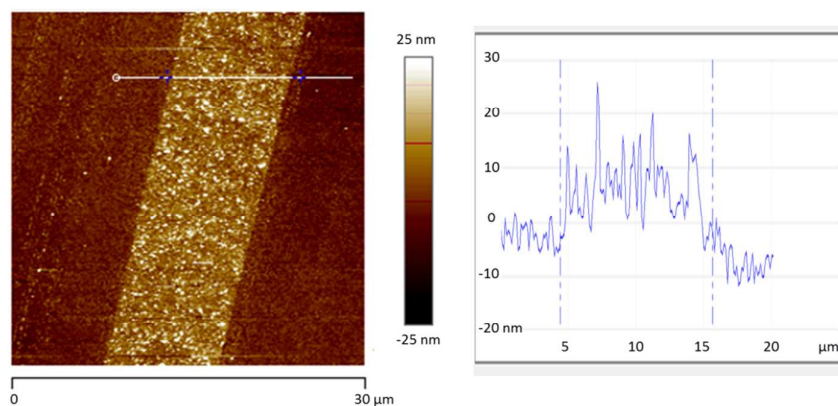


Figure S13. Left panel shows AFM height image of the WO_x@PEDOT HTL deposited on ITO. The light region indicates the WO_x@PEDOT HTL, while the dark region indicates the pristine ITO where the WO_x@PEDOT HTL was removed by knife scratching. Right panel displays a height trace, suggesting an average HTL thickness of ca. 20 nm.

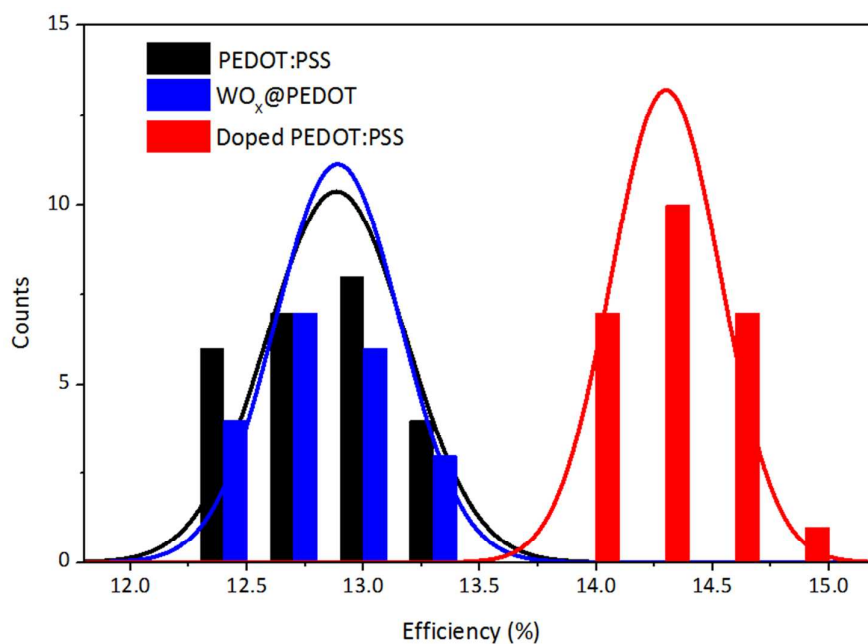


Figure S14. PCE distributions for PeSCs with different HTLs.

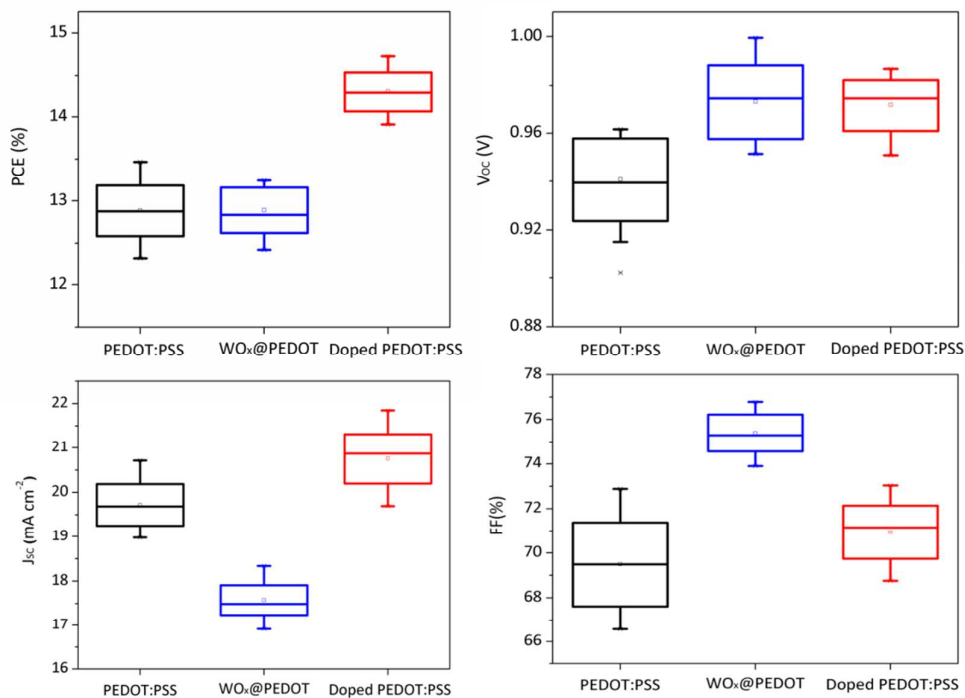


Figure S15. Histogram of PCE and V_{OC} , J_{SC} , FF of 20-25 individual solar cells under 1 sun illumination.

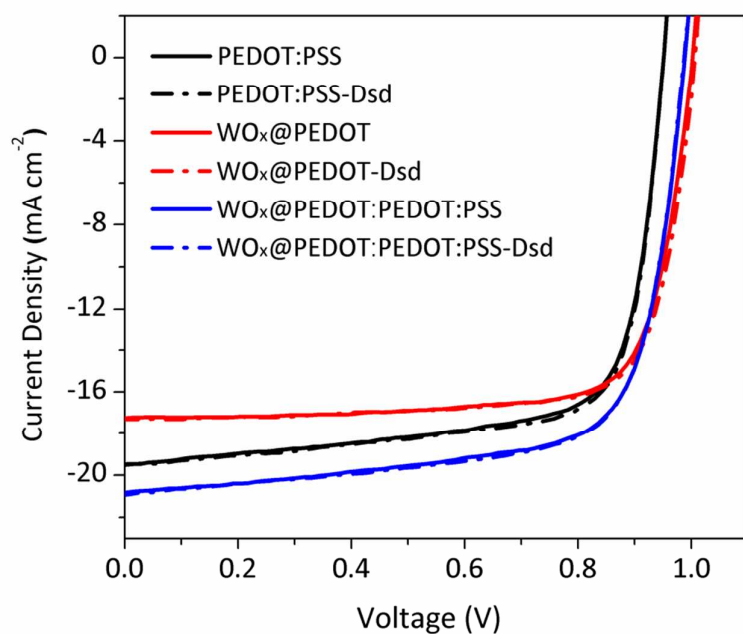


Figure S16. J - V curves of PeSCs with different HTLs with both forward (FS) and reverse (RS) scan modes under 1 sun illumination.

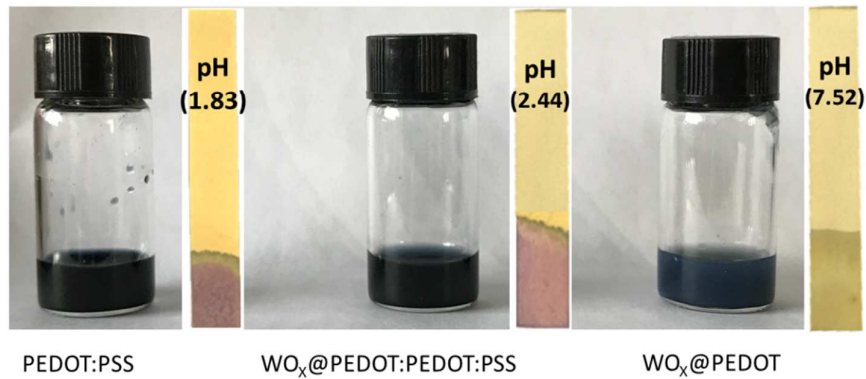


Figure S17. Photos of the samples of PEDOT:PSS, WO_x@PEDOT and WO_x@PEDOT:PSS. The insets show their PH values.